JOURNAL OF MATERIALS SCIENCE 27 (1992) 3770–3776

Synthesis and properties of model SiC–Si_3N_4 interfaces

J. J. PETROVIC, O. UNAL*, T. E. MITCHELL*
*Materials Science and Technology Division, * Center for Materials Science, Los Alamos National Laboratory, Los Alamos, NM 87545, USA*

Microscopic and macroscopic SiC–Si_3N_4 interfacial structures were synthesized and their properties examined. Microscopic interfaces were produced by hot isostatic pressing vapour–liquid–solid SiC whisker–polycrystalline Si_3N_4 matrix composites without densification aids. Macroscopic interfaces were formed by the chemical vapour deposited Si_3N_4 coating of large SiC single crystals. The characteristics of these model interfaces were investigated using transmission electron microscopy and indentation fracture. Results showed the microscopic interfaces to contain a small amount of second phase, while the macroscopic interfaces were pristine in nature with no second phase present. Pristine SiC–Si_3N_4 interfaces were strongly bonded at room temperature, but interfacial strength decreased at elevated temperatures.

1. Introduction

Interfaces are the single most important microstructural feature controlling the mechanical properties of high fracture toughness ceramic composites [1–4]. The purpose of the present investigation was to synthesize model interfaces in the SiC–Si_3N_4 system, because this system is of both fundamental and practical interest. The approach taken was to fabricate both microscopic and macroscopic SiC–Si_3N_4 interfaces in as pristine a condition as possible, in order to investigate the properties of virgin interfacial structures in this system. Microscopic interfaces involved the use of a discontinuous reinforcement in a matrix, to create a composite-like microscopic interfacial region. In this case, vapour–liquid–solid SiC whiskers were hot isostatically pressed in a polycrystalline Si_3N_4 matrix, without densification aids. Macroscopic interfaces employed single crystals, or their best approximation, to create a large-scale interfacial region. Here, a chemical vapour deposited Si_3N_4 coating was placed on a large SiC single crystal.

In the present paper, the techniques employed for synthesizing SiC–Si_3N_4 model interfaces are discussed, and some of the properties of these interfaces are presented. Elements of this work have been investigated in more detail [5].

2. Microscopic interfaces

2.1. Vapour–liquid–solid SiC whiskers

Vapour–liquid–solid (VLS) SiC whiskers developed at the Los Alamos National Laboratory are generally regarded as the highest quality SiC whiskers presently available in terms of morphology, chemistry, and substructure [6–8]. These whiskers are of high purity, and possess diameters in the range of 3–11 μm. They exhibit a low density of substructural defects in comparison to the smaller diameter (0.5 μm) vapour–solid (VS) SiC whiskers available from commercial sources. VLS SiC whiskers were employed in the synthesis of microscopic model interfaces.

2.2. Hot isostatic pressing of VLS SiC whisker–Si_3N_4 matrix composites

Because a pristine SiC–Si_3N_4 interface was sought, it was necessary to consolidate VLS SiC whiskers in a polycrystalline Si_3N_4 matrix without the use of densification aids, because these densification aids would complicate the formation of a virgin interface. Recent investigations have demonstrated that SiC whisker–Si_3N_4 matrix composites can be consolidated to a high density without the use of densification aids, by employing hot isostatic pressing (HIP) at temperatures in the vicinity of 1950 °C [9, 10].

Ube SN-E10 high-purity Si_3N_4 powder was employed for the synthesis. This powder had an average particle size of 0.5 μm (BET surface area of 10 $m^2 g^{-1}$), and was 97% α-Si_3N_4. VLS SiC whiskers were subjected to a high-speed blending operation to reduce their length-to-diameter ratio to approximately 40 μm, and then given a rigorous beneficiation treatment prior to blending with the Si_3N_4 powder, to remove metal catalyst balls and detritus associated with the VLS whisker synthesis process [11].

Si_3N_4 powder and VLS SiC whiskers were mechanically blended together in a suitable proportion to yield a 20 vol % composite material. This mixture was then uniaxially cold pressed without binders to a density of approximately 50% theoretical density, yielding pellets which were 19 mm diameter by 19 mm long. Pellets of both pure Si_3N_4 powder and the 20 vol % VLS SiC whisker–Si_3N_4 matrix composite were prepared.

Cold-pressed pellets were hot isostatically pressed using the ASEA process. This involved glass

0022–2461

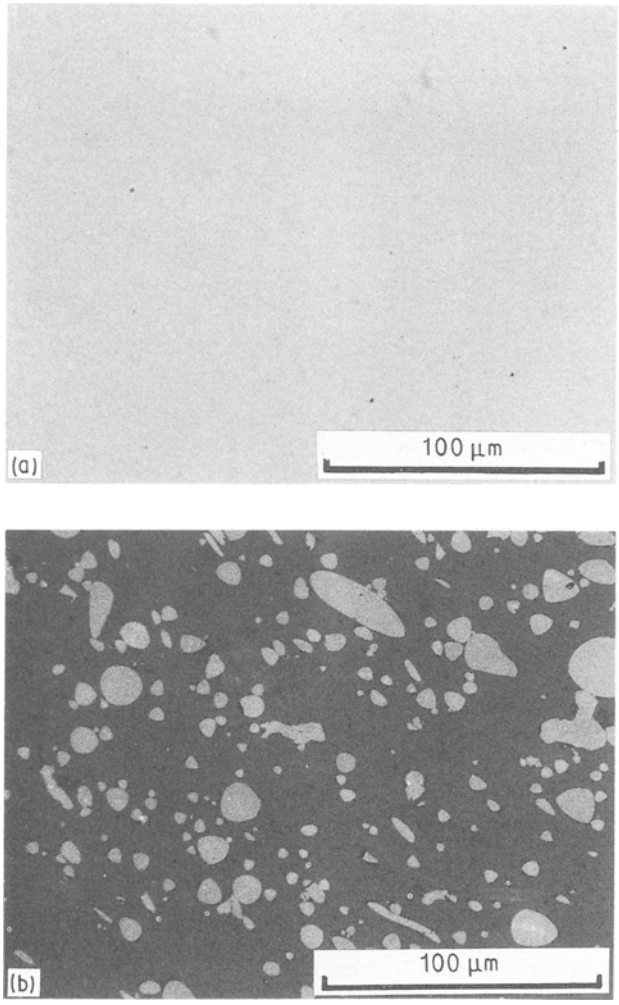

Figure 1 Optical micrographs of hot isostatically pressed (a) pure Si_3N_4 and (b) 20 vol % VLS SiC whisker–Si_3N_4 matrix composite.

encapsulation of the pellets, followed by an HIP treatment consisting of a 2 h hold at 1950 °C and 207 MPa pressure. All specimens were observed to be fully dense after the HIP consolidation. No densification additives were employed at any stage of the consolidation procedure.

2.3. Microstructural characterization

Microstructures of pure Si_3N_4 and a 20 vol % VLS SiC whisker–Si_3N_4 matrix composite densified by hot isostatic pressing at 1950 °C are shown in Fig. 1. Fully dense microstructures were indicated for both pure matrix and composite. In Fig. 1, many of the VLS SiC whiskers still possess their characteristic rounded triangular cross-sectional shape, indicating minimal diffusion effects as a result of the 1950 °C exposure. X-ray diffraction showed that the Si_3N_4 phase was totally converted to β-Si_3N_4 as a result of the HIP consolidation.

Interface specimens were prepared for transmission electron microscopy (TEM) investigations in the following general manner. Bulk specimens were cut using a slow-speed saw, mechanically polished using SiC papers down to approximately 100 μm thickness, and then dimpled with a Gatan dimpler to about 30 μm thickness. Before dimpling, 3 mm discs were cut using

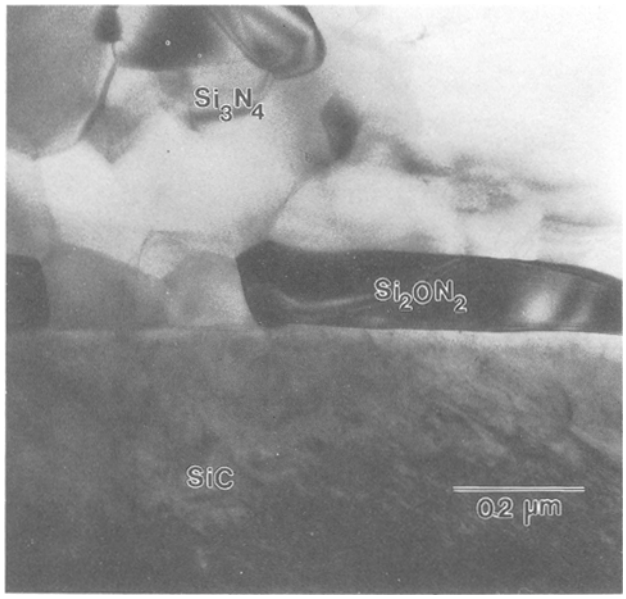

Figure 2 Bright-field transmission electron micrograph of interfacial region in the 20 vol % VLS SiC whisker–Si_3N_4 matrix composite.

a Gatan disc cutter. Preparation of electron-transparent foils was done by ion-milling, using argon gas at 5 kV in a Gatan ion-mill. TEM was performed in a Philips CM30 fitted with a Kevex 7000 energy dispersive analysis system. For lattice imaging, a Philips CM30ST electron microscope with 1.2 mm spherical aberration and a point-to-point resolution of 0.19 nm was used. Both microscopes operate at 300 kV.

A transmission electron micrograph of a typical VLS SiC whisker–polycrystalline Si_3N_4 matrix interface is shown in Fig. 2. The interface formed appeared relatively clean, although some particles of Si_2ON_2 were observed to be present at the interface. These likely result from the presence of silica on the surfaces of the starting Si_3N_4 powders and SiC whiskers. High-resolution electron microscopy (HREM) showed that SiC–Si_3N_4 interfacial regions adjacent to the Si_2ON_2 particles contained a 10 nm amorphous SiO_2 phase. A 2 nm SiO_2 interfacial phase was also noted in the pure Si_3N_4 grain boundaries. These observations suggest that the SiC whiskers originally had a thicker layer of SiO_2 on their surfaces than did the Si_3N_4 powders. The grain structure of the Si_3N_4 was observed to be roughly equiaxed in shape and submicrometre in size.

2.4. Fracture toughness

Room-temperature indentation fracture toughness measurements were performed using a 10 kg Vickers indentation, and toughness values calculated using the analyses of Anstis *et al.* [12]. Indentations in the pure Si_3N_4 and the 20 vol % VLS SiC whisker–Si_3N_4 matrix composite are shown in Fig. 3. The indentation crack pattern was particularly well formed in the pure Si_3N_4, and somewhat less so in the composite. The measured indentation fracture toughness of the pure Si_3N_4 was 2.7 MPa $m^{1/2}$, while that for the composite was 3.7 MPa $m^{1/2}$. Thus, a 40% toughening was observed for the composite material. Hardness values of

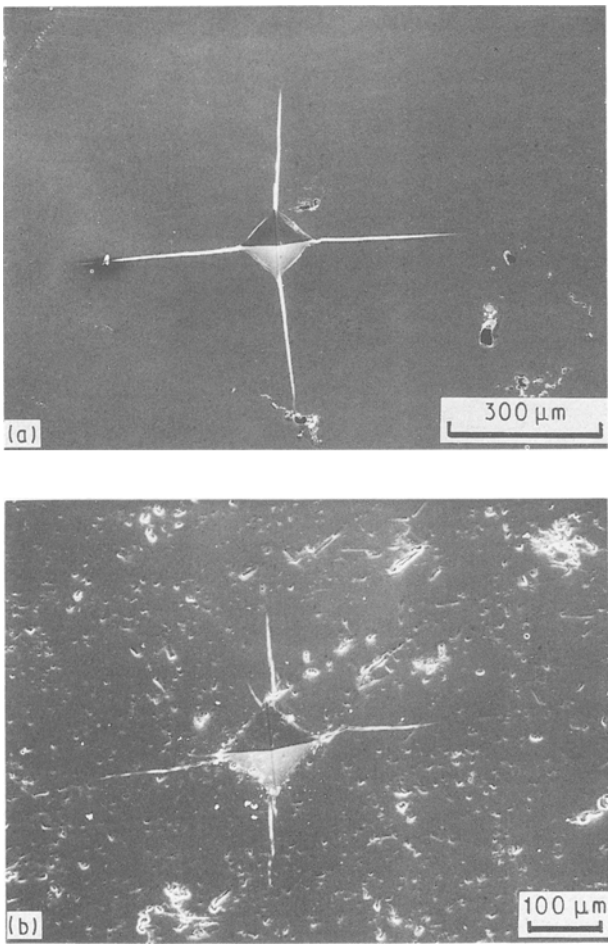

Figure 3 Optical micrographs of room-temperature microhardness indentations in (a) pure Si_3N_4 and (b) 20 vol % VLS SiC whisker–Si_3N_4 matrix composite.

pure Si_3N_4 and composite were identical, at a value of 23 GPa.

The fracture toughness value obtained for the pure Si_3N_4 densified without densification aids, 2.7 MPa $m^{1/2}$, is similar to a value of 3 MPa $m^{1/2}$ obtained by other researchers [9, 10]. This value is somewhat low in comparison to values obtained for Si_3N_4 densified using densification aids, where values in the range of 5–7 MPa $m^{1/2}$ are commonly reported. It is likely that a contributing factor to the lower Si_3N_4 fracture toughness is the strong inter-grain bonding and equiaxed nature of the β-Si_3N_4 grain structure when additives are not employed. In contrast, when additives are used the β-Si_3N_4 grains are observed to be elongated, and increased fracture toughness is attributed to this elongated grain morphology [13]. Densification aid effects on the fracture toughness of Si_3N_4 due to their presence as phase constituents in the microstructure have not yet been definitively established.

Fracture toughness of pure Si_3N_4 and the SiC whisker–Si_3N_4 matrix composite was measured as a function of temperature to a temperature of 1400 °C, using a Nikon Model QM high-temperature microhardness indentation system, and 1 kg indentation load. Results are shown in Fig. 4. The fracture toughness of pure Si_3N_4 decreased slightly with increasing

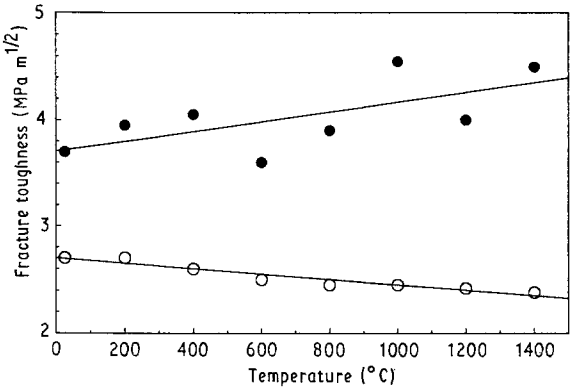

Figure 4 Indentation fracture toughness of (○) pure Si_3N_4 and (●) 20 vol % VLS SiC whisker–Si_3N_4 matrix composite as a function of temperature.

temperature, while the fracture toughness of the composite increased slightly with increasing temperature. The fracture toughness decrease for pure Si_3N_4 has been observed by others [9, 10].

In pure Si_3N_4, the indentation crack morphology changed from primarily transgranular at room temperature, to intergranular at 1400 °C. High-resolution electron microscopy indicated the presence of an approximately 2 nm width SiO_2 layer at the grain boundaries of the Si_3N_4. Softening of this thin SiO_2 grain-boundary phase at elevated temperatures is thought to be responsible for both the change in crack morphology, and the decrease in fracture toughness.

The increased fracture toughness of the VLS SiC whisker composite over that of the Si_3N_4 matrix is likely due to a combination of crack bridging [2] and crack deflection [14] toughening mechanisms. Although the fracture toughness of the composite increased with increasing temperature, the magnitude of the observed increase was not large. For VS SiC whisker–Si_3N_4 matrix composites densified without densification aids, other workers [9] have observed a slight decrease in the fracture toughness of the composite with increasing temperature.

3. Macroscopic interfaces

3.1. SiC single crystals

Relatively large, flat-faced SiC single crystals produced by the Lely sublimation process [15] were employed for the investigation. In the Lely process, high-purity polycrystalline SiC is sublimed at very high temperatures (2200 °C), with the resultant formation of high-purity SiC single crystals. The SiC crystals were green in colour, and transparent. Crystals were irregularly shaped with approximate diameters of about 5 mm, and crystal thicknesses were 0.5–1.0 mm. X-ray diffraction studies showed these crystals to be mainly the α 6H crystal structure. However, TEM studies indicated that the outer flat surfaces of the crystals were cubic β-SiC, to a depth of approximately 0.5–1.0 μm. The flat crystal faces were determined to be the cubic (1 1 1) type crystallographic planes. Such (1 1 1) planes are composed of alternate layers of silicon and carbon atoms.

3.2. Chemical vapour deposited Si_3N_4 coating of SiC single crystals

In order to form pristine SiC–Si_3N_4 macroscopic interfaces, SiC single crystals were chemical vapour deposition (CVD) coated with Si_3N_4. Prior to the coating operation, the surfaces of the crystals were cleaned by immersion in a concentrated HF solution. CVD coating of the crystals was performed at a temperature of 1500 °C and a pressure of 0.5 torr (1 torr = 1.333×10^2 Pa), using $SiCl_4$–NH_3–H_2 reaction gases at flow rates of 1, 2 and 6 l min^{-1}, respectively. The SiC crystals were mechanically supported on graphite posts in the CVD coating chamber, and the crystal and graphite post were overcoated with a thick CVD Si_3N_4 layer. Coating times of 30 h led to the formation of a 5 mm thick Si_3N_4 overcoat layer.

3.3. Microstructural characterization

CVD Si_3N_4 overcoated SiC single-crystal specimens were diamond cut to reveal the SiC–Si_3N_4 macroscopic interface. Optical micrographs of the interface are shown in Fig. 5. As may be seen, the SiC crystals did not remain monolithic after the CVD Si_3N_4 coating operation. Rather, the crystals exhibited extensive fracturing, with cracks formed perpendicular to the SiC–Si_3N_4 interface. This cracking was thermally induced upon cooling from the 1500 °C CVD temperature, due to the thermal expansion coefficient mismatch of SiC and Si_3N_4: the thermal expansion coefficient of SiC is 5.4×10^{-6} °C^{-1}, while that of Si_3N_4 is 3.3×10^{-6} °C^{-1}. Thus, in the presence of a strong interfacial bond, one would expect tensile stresses to form in the SiC and compressive stresses in the Si_3N_4. The CVD Si_3N_4 did not exhibit cracking due to the thermal expansion coefficient mismatch, as would be expected. As seen in Fig. 5, the SiC–Si_3N_4 interface in between the cracked regions was straight and well-defined, and thus amenable to structural and mechanical analyses.

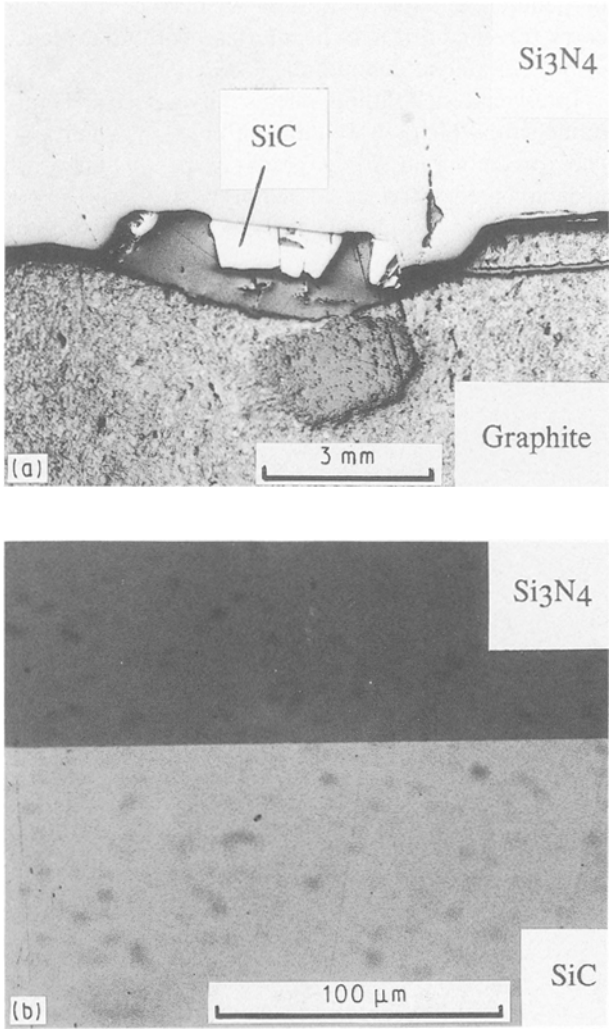

Figure 5 Optical micrographs of SiC single crystal–CVD Si_3N_4 macroscopic interface. (a) CVD Si_3N_4, with the SiC single crystal bonded to it. (b) Graphite pedestal below the SiC crystal.

3.4. Interface residual stresses

Residual stresses were estimated in the SiC crystal, using the formula developed by Chiu [16] for a coating/substrate system with a strong interfacial bond. This formula takes into account both interface planar stresses, as well as bending of the coating/substrate system, due to thermal expansion mismatch effects. For this calculation, the thermal expansion coefficients of polycrystalline SiC and Si_3N_4 given above were employed, and polycrystalline elastic moduli of 448 and 307 GPa for SiC and Si_3N_4, respectively, were used. The temperature difference was 1475 °C.

Results are shown in Fig. 6. Here, residual stress in the SiC is plotted versus the ratio of Si_3N_4 thickness/SiC thickness. As may be seen, substantial tensile stresses occur in the SiC, which increase with increasing ratio of Si_3N_4/SiC thickness. For the present case, the Si_3N_4/SiC thickness ratio was approximately 5, indicating a tensile residual stress of 544 MPa. Such a high tensile stress accounts for the cracking of the SiC single crystal. In fact, the tensile stress developed in the SiC crystal is likely to be greater than this estimate due to the fact that the coating geometry minimized stress redistribution by bending. The saturation value of residual stress in the SiC with no bending is estimated at 1380 MPa.

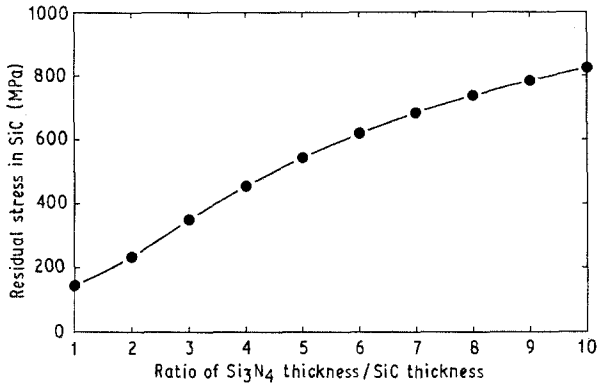

Figure 6 Calculation of residual stresses in SiC single crystal as a function of the ratio of CVD Si_3N_4 thickness/SiC crystal thickness.

Figure 7 Bright-field transmission electron micrograph of SiC single crystal–CVD Si_3N_4 macroscopic interface.

3.5. TEM of the interface

Transmission electron microscopy was performed on the macroscopic SiC–Si_3N_4 interface. Fig. 7 shows the interface at lower magnification, while Fig. 8 is a high-resolution TEM image of the interface. The CVD Si_3N_4 at the interface was observed to be α-Si_3N_4. Si_3N_4 grains at the interfacial region were columnar, with a grain size ranging between 3 and 8 μm. Also noted in the Si_3N_4 were planar faults and voids. As previously indicated, the SiC at the interfacial region was cubic in crystal structure.

The high-resolution image in Fig. 8 shows that there was no second phase present at the interface. Thus, the interface was pristine in nature, wihout the presence of any glassy phase often observed in SiC–Si_3N_4 systems, even in the HIPed composites described above.

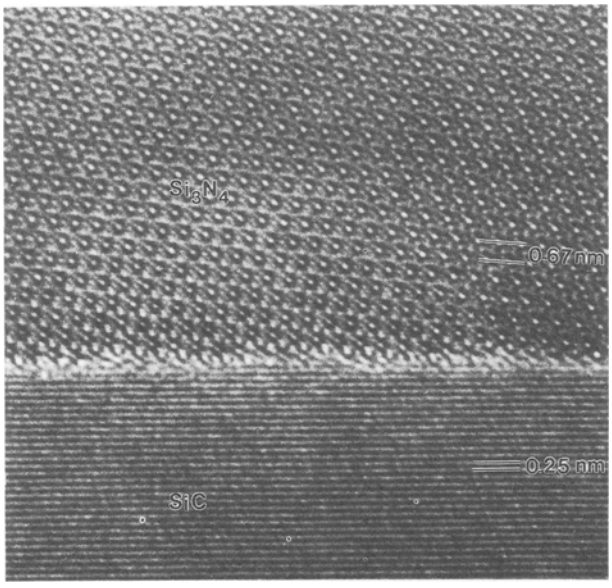

Figure 8 High-resolution electron micrograph of SiC single crystal–CVD Si_3N_4 macroscopic interface. The α-Si_3N_4 is viewed along the exact [0 0 0 1] axis, while the β-SiC is viewed along a (1 1 1) plane close to the [1 1 0] axis.

Because the interface was pristine, it was possible for interfacial orientation relationships to develop during deposition. Two prominent orientation relationships were, in fact, observed: $(1\,0\,\bar{1}\,0)Si_3N_4//(1\,1\,\bar{1})SiC$, $[0\,0\,0\,1]Si_3N_4//[1\,0\,1]SiC$; $(1\,0\,\bar{1}\,0)Si_3N_4//(1\,1\,\bar{1})SiC$, $[1\,\bar{2}\,1\,0]Si_3N_4//[1\,0\,1]SiC$. However, small angular deviations (2–6°) were commonly observed from these exact orientation relationships.

3.6. Microhardness indentation at the interface

As indicated by the TEM analyses, the macroscopic SiC–Si_3N_4 interface was pristine in nature. Some initial microhardness indentation experiments have been employed to examine its fracture response. Fig. 9 shows a 1 kg Vickers room-temperature indentation positioned so that one of its diagonals lay approximately in the plane of the interface. As may be seen, no diagonal cracks were produced in the interface itself. This is an indication that the interface was a very strong one at room temperature. The effects of tensile residual stresses and crystallographic anisotropy on the indentation crack pattern in the SiC are evident in Fig. 9. In Fig. 10, a 1 kg room-temperature Vickers indentation was positioned in the SiC, in order to drive a radial indentation crack to the interface at a perpendicular angle of attack. As may be seen, this crack travelled through the interface, with no evidence of any interfacial debonding.

Interfacial debonding effects have been recently modelled by He and Hutchinson [17, 18]. Their analysis predicts that, for a crack perpendicularly approaching an interface in materials with somewhat similar elastic moduli, interfacial debonding will occur

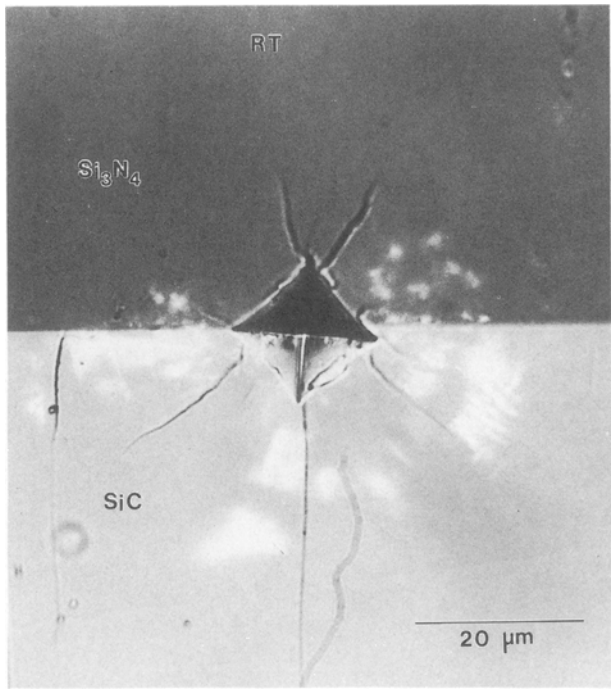

Figure 9 Optical micrographs of room-temperature Vickers indentation positioned in the plane of the macroscopic SiC–Si_3N_4 interface.

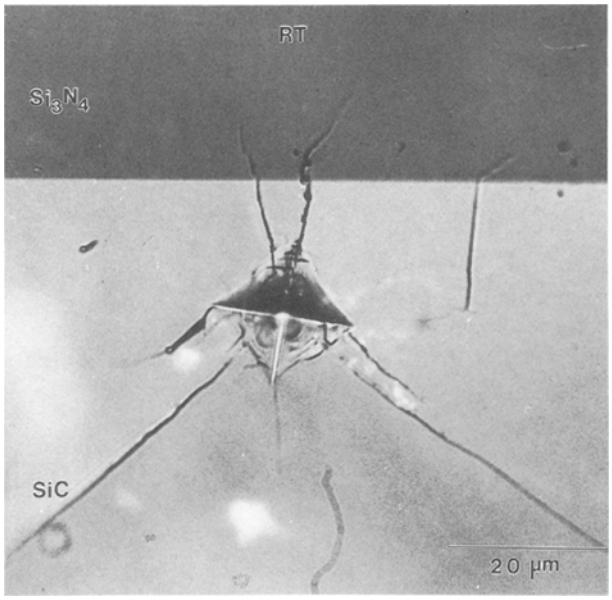

Figure 10 Optical micrograph of room-temperature Vickers indentation in the SiC portion of the SiC–Si_3N_4 macroscopic interface, positioned for the indentation crack to intersect interface at a perpendicular angle of attack.

when the ratio of interface fracture energy/non-interface fracture energy is less than 0.25. The present indentation observations for the macroscopic SiC–Si_3N_4 interface indicate that, at room temperature, the ratio of SiC–Si_3N_4 interfacial fracture energy/Si_3N_4 fracture energy is greater than 0.25, because no interface debonding was observed.

However, preliminary results suggest that the SiC–Si_3N_4 interfacial fracture energy decreases with increasing temperature. Fig. 11 shows a 1 kg Vickers indentation placed in the Si_3N_4 phase in the vicinity of the macroscopic SiC–Si_3N_4 interface at a temperature of 1200 °C, using a high-temperature microhardness indentation. Although the indentation and its associated crack pattern is not particularly well-formed, it is evident that a perpendicular crack has clearly debonded the interface. Thus, this preliminary result indicates that the SiC–Si_3N_4 interfacial fracture energy is less than 0.25 of the fracture energy of SiC at 1200 °C.

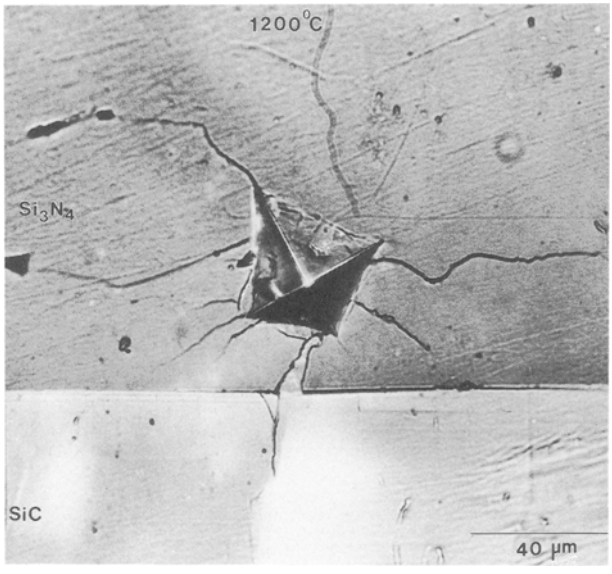

Figure 11 Optical micrographs of Vickers indentation placed in the Si_3N_4 portion of the SiC–Si_3N_4 macroscopic interface at 1200 °C.

4. Conclusion

Microscopic and macroscopic model SiC–Si_3N_4 interfaces were synthesized and their properties initially evaluated. Microscopic interfaces were produced by hot isostatically pressing composites of VLS SiC whiskers in a matrix of polycrystalline Si_3N_4 without the use of densification aids. Macroscopic interfaces were synthesized by placing CVD Si_3N_4 coatings on SiC single crystals.

Microscopic interfaces in VLS SiC whisker–Si_3N_4 matrix composites were observed to be relatively clean, although the presence of isolated Si_2ON_2 particles and a thin (10 nm) SiO_2 layer was noted. The indentation fracture toughness of pure Si_3N_4 densified without additives was 2.7 MPa $m^{1/2}$ at room temperature, and decreased slightly with increasing temperature. The fracture toughness of the composite was 3.7 MPa $m^{1/2}$ at room temperature, and increased slightly with increasing temperature. Fracture toughness behaviour was interpreted in terms of interfacial properties.

SiC single crystals CVD coated with Si_3N_4 were observed to be cracked due to thermal expansion coefficient mismatch thermal stresses. High-resolution electron microscopy showed the macroscopic SiC–Si_3N_4 interfaces to be pristine, with no evidence of any interfacial phases present. Orientation relationships between the SiC crystal and the CVD Si_3N_4 were determined. Microhardness indentation experiments indicated a high SiC–Si_3N_4 interfacial fracture energy at room temperature, but suggested a decrease in this interfacial energy with increasing temperature.

Acknowledgements

The authors thank the DOE Office of Basic Energy Sciences, Division of Materials Science for support of this investigation. The authors are grateful to Professor Robert F. Davis, North Carolina State University, for supplying the Lely SiC single crystals. The services of ABB Autoclave Systems, Inc. for hot isostatic pressing, and Union Carbide Advanced Ceramics for CVD coating are acknowledged.

References

1. A. G. EVANS, *J. Amer. Ceram. Soc.* **73** (1990) 187.
2. P. F. BECHER, C. H. HSUEH, P. ANGELINI and T. N. TIEGS, *ibid.* **71** (1988) 1050.
3. A. G. EVANS, M. Y. HE and J. W. HUTCHINSON, *ibid.* **72** (1989) 2300.
4. H. C. CAO, E. BISCHOFF, O. SBAIZERO, M. RUHLE and A. G. EVANS, *ibid.* **73** (1990), 1691.
5. O. UNAL, PhD thesis, Case Western Reserve University (1991).
6. J. J. PETROVIC and G. F. HURLEY, in "Fiber Reinforced Ceramic Composites", edited by K. S. Mazdiyasni (Noyes Publications, Park Ridge, New Jersey, 1990) p. 93.

7. S. R. NUTT and D. S. PHILLIPS, in "Proceedings of the Conference on Interfaces in Metal-Matrix Composites", New Orleans, March 1986, edited by A. K. Dhingra and S. G. Fishman (The Metallurgical Society, Warrendale, Pennsylvania, 1986) p. 111.
8. T. N. TAYLOR, *J. Mater. Res.* **4** (1989) 189.
9. G. PEZZOTTI, I. TANAKA, T. OKAMOTO, M. KOIZUMI and Y. MIYAMOTO, *J. Amer. Ceram. Soc.* **72** (1989) 1461.
10. I. TANAKA, G. PEZZOTTI, T. OKAMOTO, Y. MIYAMOTO and M. KOIZUMI, *ibid.* **72** (1989) 1656.
11. F. D. GAC, PhD thesis, University of Washington (1988).
12. G. R. ANSTIS, P. CHANTIKUL, B. R. LAWN and D. B. MARSHALL, *J. Amer. Ceram. Soc.* **64** (1981) 533.
13. F. F. LANGE, *ibid.* **62** (1979) 428.
14. K. T. FABER and A. G. EVANS, *Acta Metall.* **31** (1983) 565.
15. J. A. LELY, *Ber. Deut. Keram. Ges.* **32** (1955) 229.
16. C. C. CHIU, *J. Amer. Ceram. Soc.* **73** (1990) 1999.
17. M. Y. HE and J. W. HUTCHINSON, *Int. J. Solids Struct.* **25** (1989) 1053.
18. *Idem., J. Appl. Mech.* **56** (1989) 270.

Received 18 March
and accepted 1 July 1991